Design and Performance of Earth Retaining Structures

Sponsored by the
Geotechnical Engineering Division
of the
American Society of Civil Engineers

In cooperation with the
Ithaca Section, ASCE

Cornell University
Ithaca, New York
June 18-21, 1990

Geotechnical Special Publication No. 25

Edited by
Philip C. Lambe
and Lawrence A. Hansen

THE BEHAVIOR OF BRIDGE ABUTMENTS ON CLAY

Malcolm D. Bolton[1], Sarah M. Springman[2] and H. Wing Sun[3]

ABSTRACT: Aspects of the behavior of bridge abutments on clay have been simulated in small-scale centrifuge models. Data of two contrasting tests are presented. One shows the behavior of a full-height abutment with a spread base over firm to stiff clay, during backfilling, deck loading, and subsequent clay consolidation. The other investigates the lateral loading effect of embankment surcharge on pre-driven piles, such as might be used to support an abutment on softer clay. A simplified deformation mechanism captures approximately the observed patterns of undrained lateral movements. This can form the basis of a design method which accounts properly for soil-structure interaction.

INTRODUCTION

A recent statistical study for FHWA (3) of bridge abutments in North America concluded that lateral movements at the bridge deck connection were much more significant than vertical movements in determining whether the structure remained serviceable. Limits of 100 mm vertical movement and 50 mm horizontal were thought to be applicable to a wide range of bridge deck and abutment types. Unfortunately, there is a lack of fully instrumented tests from which calculation methods for lateral movements could have been derived. Furthermore, the most typical scenario leading to unserviceability involved both horizontal and vertical movements of bridge deck supports. Clay soils were most frequently cited as the seat of damaging movements, but the reports of damage involved shallow and deep foundations in equal numbers. Apparently, the likelihood of lateral movement for piled bridge abutments over weaker soils is similar to that for abutments on spread footings over stiffer soils.

The source of these movements, and the means for their prediction, is explored below with respect to full-height abutments of the type shown in figure 1, (a) with a spread base, (b) on piles.

---

1 - Lecturer, 2 - Research Fellow, 3 - Research Student, Cambridge University Engineering Department, Trumpington Street, Cambridge, CB2 1PZ, England.

Figure 1. Full-Height Bridge Abutments
(a) Spread Base (b) Piled Base

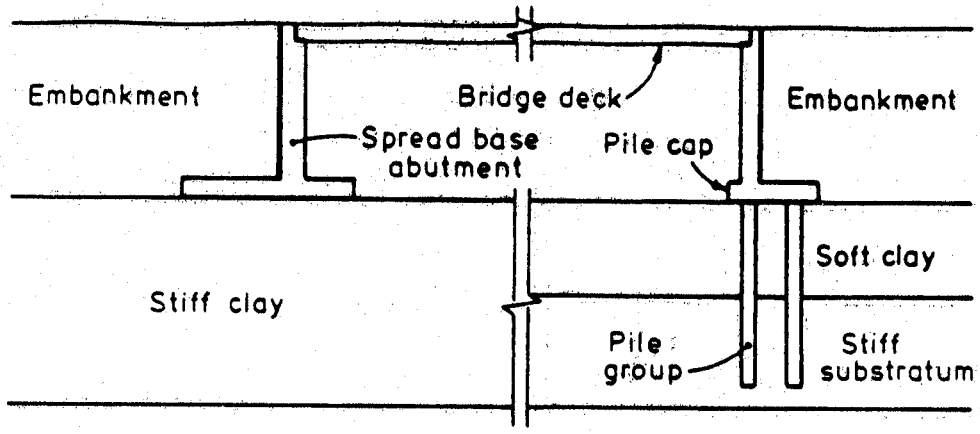

CENTRIFUGE TEST METHOD

The principles of centrifuge testing are now well known (6). When the scale of a model is reduced by a factor n and its "self-weight" increased by the same factor in a centrifuge, the distribution of vertical stresses in an equivalent field scale prototype, made of identical materials, is correctly replicated. If, in addition, the model boundaries are sufficiently remote from the focus of interest, or themselves simulate field boundaries, then the complete response to some desired stimulus can be determined from the behavior of the model. Applicable scaling factors are listed in table 1.

Table 1. Scaling Factors Multiplying Centrifuge Model Parameters

Length		n		
Stress, pressure, strength		1		
Strain, rotation		1		
Displacement		n		
Consolidation time		n^2		
Bending stiffness	per pile	n^4	per m	n^3
Bending moment	per pile	n^3	per m	n^2

Two sets of criteria must additionally be satisfied before the modelling can be accepted as valid. First, deviations from the ideally uniform body force field must be reduced to acceptable levels. In the tests to be described the variation in "gravity" at different centrifuge radii causes stress deviations of less than 3%, and the inclination of the body force due to curvature is less than 5% in the zones of soil which interact with the structures. These favourably small errors are due to the relatively large working radius (4 m) of the Cambridge Geotechnical Centrifuge: figure 2.

Figure 2. Outline of a Model on the Cambridge Beam Centrifuge

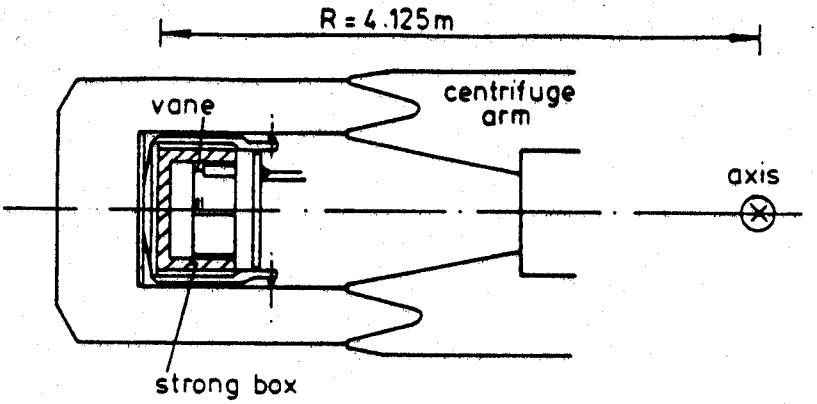

Second, the stress history of the soil in the model should replicate that in the desired prototype. Our approach to the ideal was to aim for realistic soil densities and strengths, but to accept that geological processes and construction methods could not be modelled directly. The equipment consisted of a liner (200 x 675 mm in plan) in which the pre-existing soil strata (clay over sand, for example) could be prepared, a consolidometer which could receive the liner and subject these soils to any desired overconsolidation cycle, and a strong box with a stiff, lubricated Perspex window, which could hold the liner in a centrifuge test up to 100g. The soil could then be brought into equilibrium with the desired water table set by an overflowing standpipe, permitting swelling or re-consolidation to take place. Finally, it was possible to conduct a model site investigation, in flight, to demonstrate that the required soil strength profile had been achieved. Figure 3 shows a typical vane test and undrained strength profile for 200 mm of kaolin clay in test HWS7 (referred to later), representing 20 m depth at 100g.

Figure 3. Vane Strength Profiles at 100g

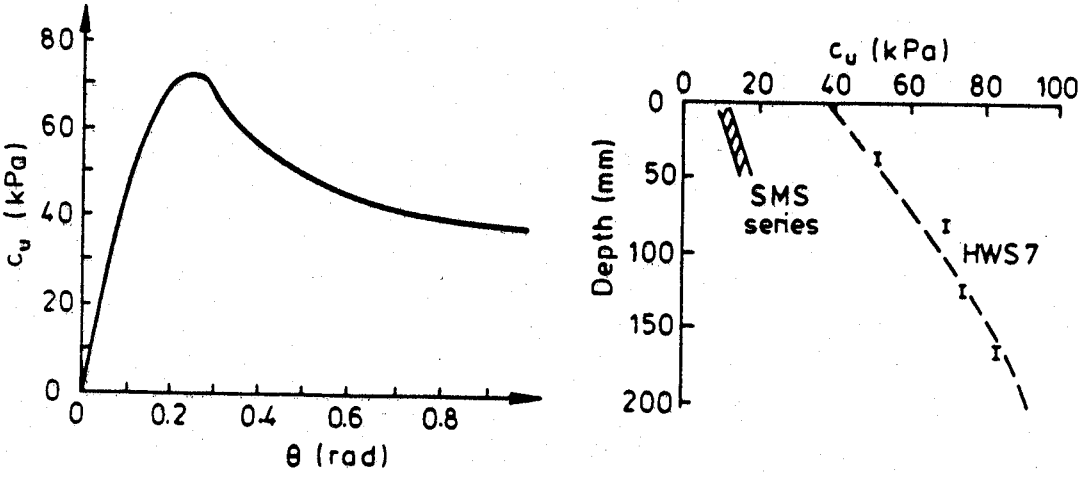

ABUTMENT ON SPREAD FOUNDATION

Test HWS7 is one of a sequence aimed at investigating the soil-structure interaction of bridge abutments founded directly over firm to stiff clay. Kaolin slurry was consolidated, as described earlier, over a period of about 1 month. A staged load-unload cycle was used to create a firm clay block into which pore pressure transducers could be inserted and backfilled. The block was then taken to its maximum consolidation pressure of 660 kPa before swelling in stages to 66 kPa. Excess water was then removed, the consolidometer opened, and the soil was trimmed to shape inside the liner which was then slid into the strongbox. The back surface of the clay was forced against the greased box, while the front surface was marked with a matrix of black plastic bullets within a painted grid, which were used to measure subsoil displacements from photographs taken through the Perspex window in flight.

The aluminium alloy wall was intended to model at 1/100 scale a plane strain section of abutment wall retaining 8 m of granular backfill. The 5.5 mm thickness modelled the bending rigidity of a 1 m thick reinforced concrete prototype. Figure 4 details the locations of wall instrumentation: in (a) the 13 fully active strain gauge bridges used as bending moment transducers (bmts) on both stem and base, and in (b) the 7 linear variable differential transformers (lvdts) used to indicate wall movement, together with 1 to show any soil heave in front of the base. These measurements are projected in terms of the vertical and horizontal displacement, and rotation, of a reference point (Figure 4 b) taken at the stem-base junction.

A deck-load simulator was designed to investigate the effects of the installation of a bridge deck resting on the top of the abutment, and the subsequent passage of heavy vehicles. Two Rolafram jacks bore on vertical, strain-gauged, brass rods which were fitted at both ends with spherical bearings to minimise the inclination and eccentricity of vertical thrust transmitted down to the wall crest.

Figure 5 shows a view of the model wall in place, relative to the sand hopper which was used to deposit dense granular fill behind the wall in flight. This construction was performed once the clay had come fully into equilibrium at 100 g with its imposed piezometric level, and following the taking of an in-flight vane probe such as that shown in figure 3. A medium and uniformly sized, sub-rounded, dry silica sand (Leighton Buzzard 30/52) was poured in 11 layers to form an 80 mm high embankment behind the wall. Each pour lasted 0.3 s and the interval between layers was 20 s, so the whole construction period of 200 s corresponded to 23 days at full scale. The high relative velocity of the sand grains as they struck the accumulating fill created a relative compaction of 97% (modified Proctor), with a dry unit weight of 16.5 kN/m^3 taken from mass and profile measurements after the test. Overall height was controlled within ±5%, and the depth of soil above the top surface of the wall base in HWS7 was 75 mm ± 4 mm.

Figure 4. Instrumentation Around the Wall

a) Bending Moment Transducers

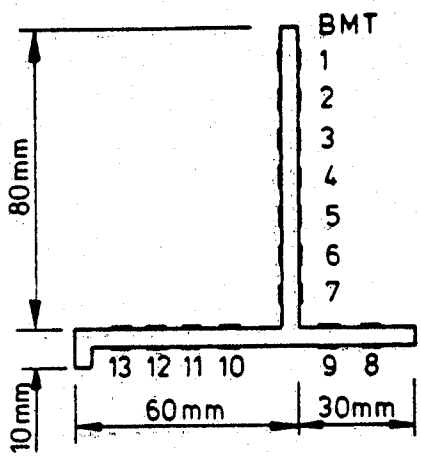

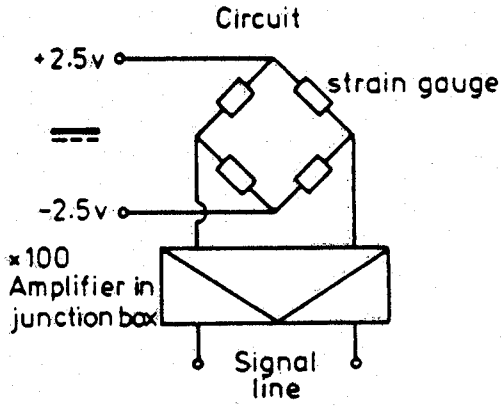

b) Displacement Transducers

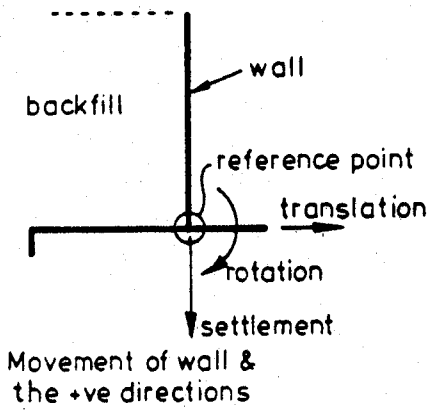

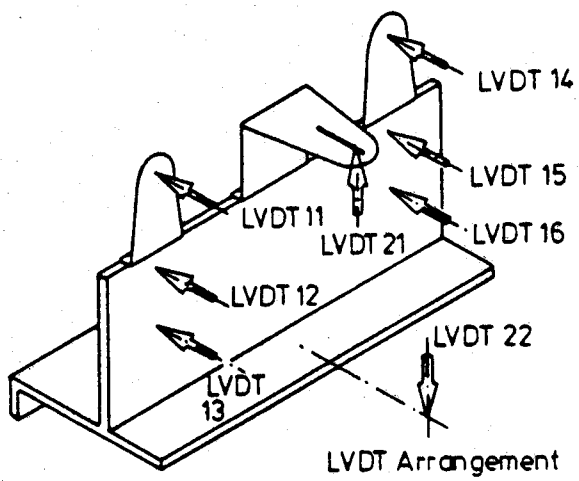

Figure 5. General Arrangement of Model HWS7

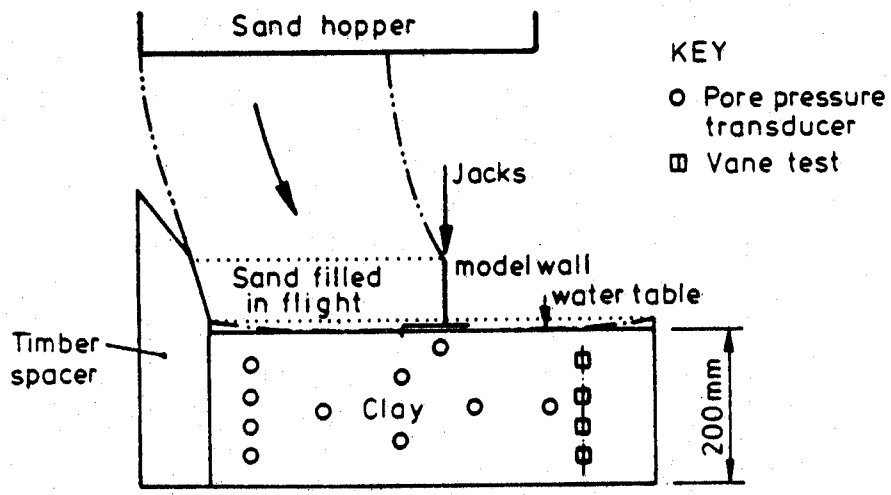

Embankment construction caused an immediate heave, forward translation and backward rotation of the reference point on the stem-base junction, corresponding to an instantaneous rotation about a high center, see figure 6a. For the next 36 minutes (250 days, prototype) consolidation of the underlying clay magnified the lateral displacement mode and permitted general settlement: see figure 6b. The time histories of base translation, settlement and rotation, and bending moments near the junction, 10 mm up the wall stem, and 8 mm along the toe, are shown in figure 7. The initial period of embankment building led to a tendency for outward movement of the wall base, permitting pressures in the accumulating fill to remain close to fully active. Subsequent consolidation with the fill in place led to a tendency for inward rotation which was strongly resisted by the fill: earth pressure increments high on the stem caused bending moments to rise, but the stiffness of the fill kept the point of rotation high, so the base continued to move outwards.

Figure 6. Wall Displacements (Magnified Scales): Test HWS7
a) After Construction b) After 36 minutes

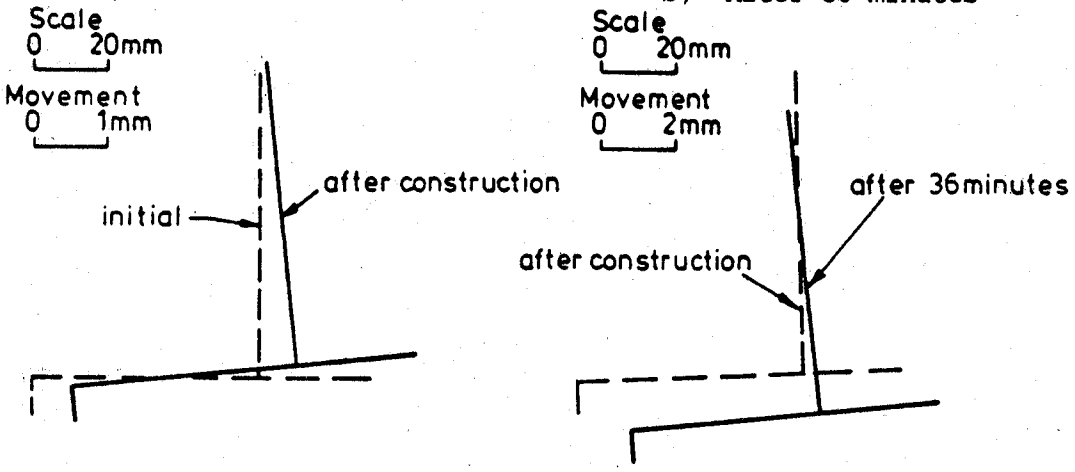

Figure 7. Time Histories: Test HWS7

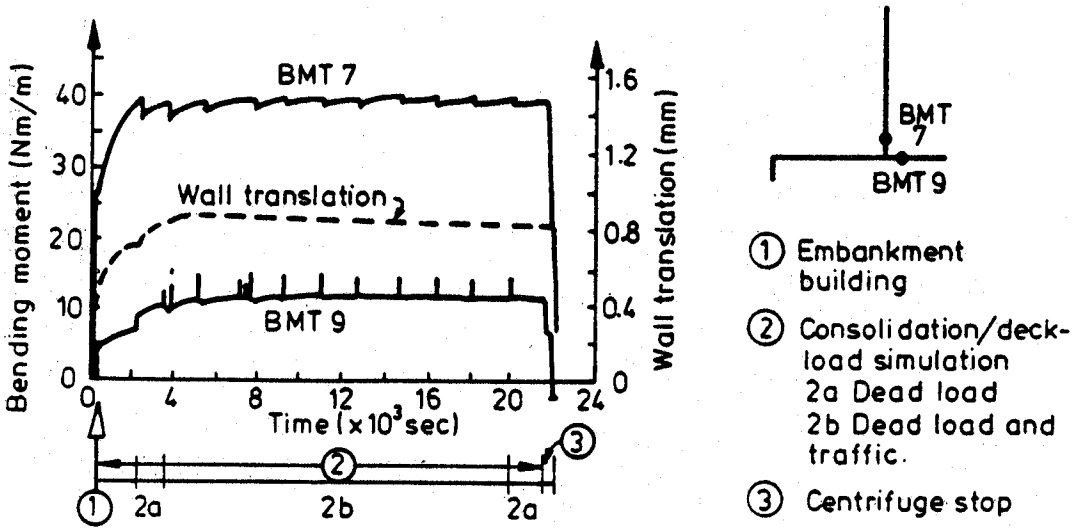

Figure 7 shows that following construction and the first 36 minutes of consolidation, certain bridge loading effects were simulated. A vertical load of 240 N (120 kN/m, prototype) was first applied to represent the dead weight of the deck. This was left to consolidate for a further 24 minutes (168 days, prototype). A second increment of load, equal to the first, was then successively applied and removed in 15 cycles with a duration of about 10 s (1 day prototype) to simulate traffic effects. As the vertical load exceeded its past maximum, the rates of backward rotation, forward translation and settlement all increased, the net effect of which was apparently to permit lateral earth pressures to fall slightly. Subsequent unloading-reloading cycles had little effect on the wall stem, though the bending moments in the base continued to reflect the cyclic changes of thrust in the stem.

Through all these stages it became clear that the changes of lateral earth pressure due to consolidation in the underlying clay could be at least as significant as those induced on backfilling and by deck loading. In terms of prototype displacements, however, the ultimate settlement of 93 mm, coupled with a base translation of 93 mm, and sufficient backward rotation to exactly eliminate horizontal movement at the elevation of the deck, fall within FHWA limits (3). If earth pressures can be safely predicted, spread bases could be acceptable for abutments on firm to stiff clays.

LATERAL LOADING OF PILES DUE TO EMBANKMENT CONSTRUCTION

If unacceptable lateral displacements have been observed in piled abutments of the form shown in figure 1b, it presumably follows that greater attention should have been paid to lateral loading of the piles, including the effects of softer superficial clays being squeezed against piles under the influence of the embankment surcharge. This mechanism has been investigated (7) in a series of centrifuge tests conducted at 100g on 1/100 scale models of idealised prototypes consisting of one or two rows of piles. The particular test described here is SMS7 in which a single row of 5 free-headed piles, diameter d = 12.7 mm (1.27 m, prototype), spacing s = 40 mm (4 m, prototype) s/d = 3.15, which have been driven through a 60 mm deep soft clay layer into a 100 mm deep sand layer (6 and 10 m prototype, respectively): figure 8. To simplify the embankment loading condition, surcharge was applied adjacent to the piles using a tailored latex rubber bag in contact with the clay, constrained on its other five sides, and capable of being pressurised to a measured air pressure.

The piles were made from 12.7 mm diameter 18SWG aluminium alloy tubing and were 300 mm long, fully penetrating the model soils, into which they were driven with the aid of a conical shoe. The bending stiffness of the pile was comparable to a solid reinforced concrete pile of the same diameter. Each pile was externally strain gauged with 8 half-bridge bending moment transducers, which were protected by an acrylic moisture barrier and two layers of shrinkfit plastic tubing. Signals were balanced and amplified on the model package.

Figure 8. General Arrangement of Model SMS7

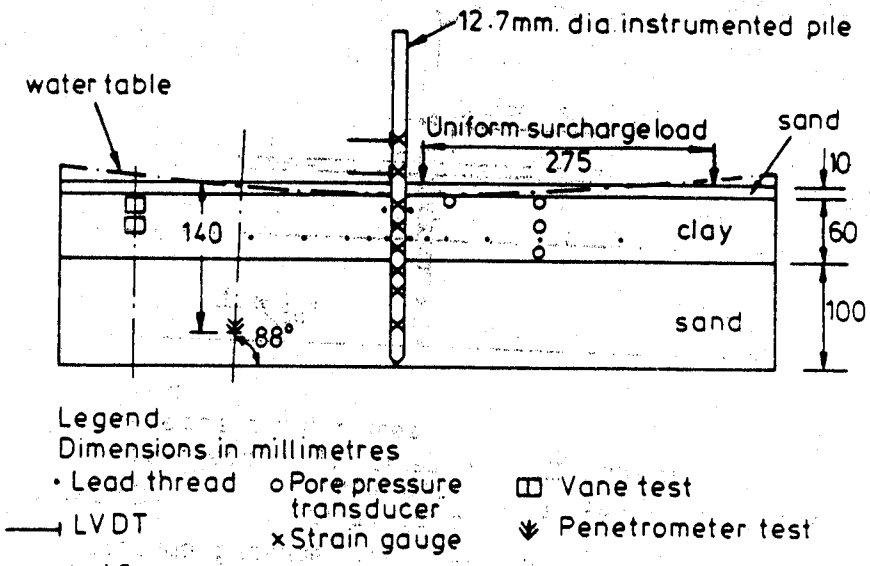

The centrifuge package was identical to that described earlier. The same soils were also used, but with a different consistency. Preparation in the liner began with the dry pouring of a 100 mm layer of medium loose Leighton Buzzard sand, followed by its slow saturation by upward flow of water. Weighings before and after this process indicated an average relative density of about 60%. The kaolin slurry was then placed in the liner which had been inserted inside the consolidometer. After an initial, staged, consolidation cycle to facilitate the insertion of pore pressure transducers, the consolidation pressure was taken to its maximum value of 86 kPa. The liner was removed three days before the centrifuge flight and trimmed to a total soil depth of 160 mm.

The liner was then slid inside the greased strongbox and the window was attached. The model piles were installed at 1g, before the loading apparatus and site investigation gear were assembled. This did not exactly replicate stress-strain conditions at full scale but comparisons between piles inserted at 1g and in flight have shown lateral capacity variations of only about 10% (2).

The final operation was temporarily to remove the window, so that markers could be placed as described earlier. In addition, horizontal lead threads were inserted using a hypodermic needle, parallel to the row of piles, so that internal deformations could be obtained from radiography after the test. The package was then re-assembled and a 10 mm layer of sand was placed over the soft clay, so as better to define its surface.

The pore pressures, which are initially negative after removal from the consolidometer and storage during model making, increased on testing at 100 g due to the increase in total vertical stress. After 2 hours (2.3 years, prototype) the pore pressures had come into equilibrium with the imposed groundwater level indicated on figure 8. The investigation of surcharge loading effects could then begin.

The surcharge was increased to 19 kPa and then by nominal 20 kPa intervals up to 93 kPa. A complete unload-reload loop was then followed. Each loading stage was held for about 2 minutes (14 days, prototype) during which a photograph was taken : the re-attainment of 93 kPa was held constant for 30 minutes (0.57 years, prototype) so that vane tests could be carried out.

Vane tests were conducted on the far side of the piles from the surcharge. The range of data from all the tests with a similar stress history is shown on figure 3. The peak shear strength increased from about 11.5 kPa at a depth of 10 mm (1 m, prototype), up to about 16.5 kPa at 50 mm (5m, prototype).

On completion of the vane tests, surcharge loading was continued in nominal 20 kPa increments with unload-reload loops at 152 and 189 kPa, by which time the clay was beginning to be squeezed under the edge of the bag housing and past the piles. At this point the test was stopped. Evidence from the period of constant surcharge during vane testing indicated that the changes of pile bending moments during loading were much more significant than subsequent changes as the clay consolidated under a load increment. Ideally, the interpretation of the effect of a load increment should be in terms of the undrained strength of the clay operative when the load was applied, taking consolidation into account.

A best-fit polynomial was drawn through the bending moment data points, imposing zero values at the pile's free ends: figure 9a. Datum values were taken as those immediately before surcharging started. By double differentiation and double integration of the bending moment polynomial, the net lateral pile pressure (figure 9b) and the relative pile deflections (figure 9c) were calculated. The lateral pressures, derived by double differentiation of fitted data points, should be taken as approximate. The distinction between action on the pile in the soft layer and reaction provided for the pile in the stiff layer is, however, clear. The lvdts at the pile head could only fix position (not rotation). Absolute pile displacements were plotted by assuming that the pile tips did not displace. The inference from figure 9c is that although the embedded length of the piles in the sand was too small for them to be considered fully fixed, the majority of pile head displacement was still due to pile curvature rather than tip rotation. It will be seen that the maximum bending moment occurred about 25 mm or two diameters below the clay-sand interface, and that it increased roughly in proportion to the surcharge.

Equivalent full-scale piles would deflect 56 mm at their crest, and have a maximum bending moment of 2.2 MNm, at a surcharge of 152 kPa corresponding approximately to an 8 m high embankment. This would generate acceptable bending strains, up to 0.26×10^{-3} in the 1.27 m diameter piles. Of course, abutment designers must also allow for the effects of a stiff pile cap, and the lateral thrust of the backfill, each of which will modify the bending moment profile compared with that observed in the experiment. The objective of the model test was to investigate lateral loading on the piles due to soil squeeze, under a simple set of boundary conditions.

Figure 9. Data from the Center Pile, Test SMS7
a) Bending Moment Nm b) Lateral Pressure kPa c) Deflection mm

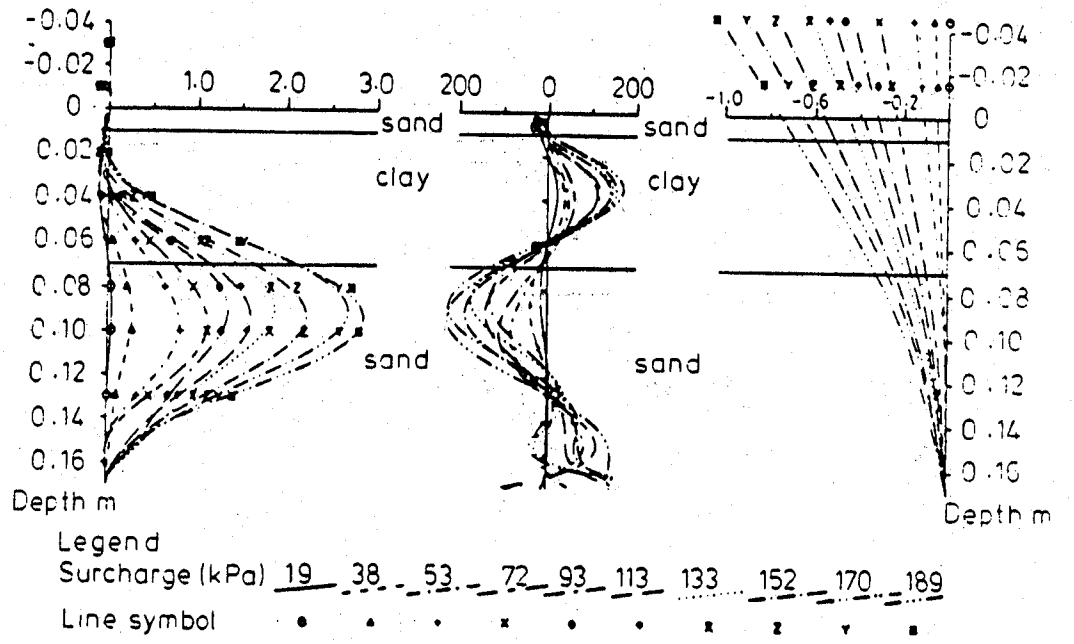

GEO-STRUCTURAL MECHANISMS

Three conditions are to be applied in the solution of problems in solid mechanics: equilibrium, compatibility and material deformability. When applied in terms of stresses and strains at a point, some means has to be found of integrating these expressions to satisfy arbitrary boundary conditions of force or displacement. This can be achieved using the principles of continuum mechanics as embodied in the finite element method. The FE program CRISP has been used (8) to analyse the transient response of an abutment wall on clay due to sequential backfilling. Computed wall displacements were qualitatively similar to those of HWS7 in figure 6, but great attention had to be paid to the parameters describing the non-linear stress-strain relations if correct magnitudes were to be derived. Practising engineers often reject FE analyses for routine design, when they recognise that the results are highly sensitive to the values assumed for input parameters with which they are unfamiliar. A similar rejection may follow if the crucial behavior mechanisms are obscured by unnecessary detail.

An alternative approach, used widely in structural mechanics, is to apply equilibrium and compatibility conditions not at every point but in a global idealization for a particular element. For example, engineers' beam theory usually ignores stress concentration at supports and beneath loads, and neglects deflection due to shear.

This structural mechanics approach has been effective in enabling engineers to design structures which deform tolerably. A similar approach will be used here to shed some light on the design of serviceable bridge abutments.

We will consider just one aspect of the larger problem: the immediate undrained lateral soil movements which must occur beneath the edge of a block of vertical surcharge. Figure 10 shows in (a) the stress increments and in (b) the soil displacements, which comprise a simplified geo-structural mechanism. The vertical plane OV is considered frictionless, and displacements beneath the planes AV and PV (inclined at 45°) are neglected. These assumptions are both consistent with the adoption throughout the deforming region of vertical and horizontal principal directions.

Figure 10. A Geo-Structural Mechanism for Undrained Surcharge

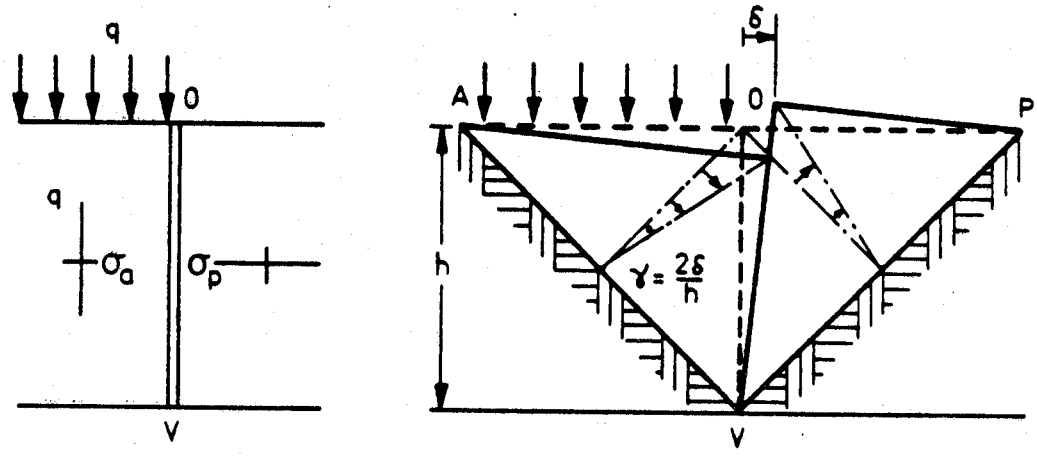

A further simplification is to imagine that the real soil is replaced by a homogeneous isotropic material with properties similar to those at mid-depth of the actual stratum, and possessing an initial earth pressure coefficient of unity. Let the increments of horizontal stress σ_h in AOV and POV be σ_a and σ_p: if the plane OV is to remain in equilibrium with zero external forces, then these horizontal stress increments must be equal. The increase in mobilized shear strength is half the increase in deviatoric stress, that is $\frac{1}{2}(q - \sigma_h)$ in active zone AOV and $\frac{1}{2}\sigma_h$ in passive zone POV.

If point O is taken to displace by δ horizontally and δ vertically then the shear strain in both deforming triangles must be $\gamma = 2\delta/h$, where h is the depth of the clay. If the shear strains are the same then so must be the shear stresses, if the soil is isotropic, so that $c_{mob} = q/4$. Figure 11 shows data of normalised undrained shear stress versus strain for kaolin tested in plane compression at OCRs of 10 and 3.3, corresponding to one third full depth in HWS7 and SMS7 respectively. Tests at OCRs of 7 and 2 for mid-depth would have been more ideal. Applying this data to test HWS7 we get $q = 7.5 \times 16.5 = 124$ kPa, so $c_{mob} = 31$ kPa. Now $c_u = 70$ kPa at mid-depth, so

Figure 11. Mobilization of Undrained Shear Strength of Kaolin (Powrie, 1986)

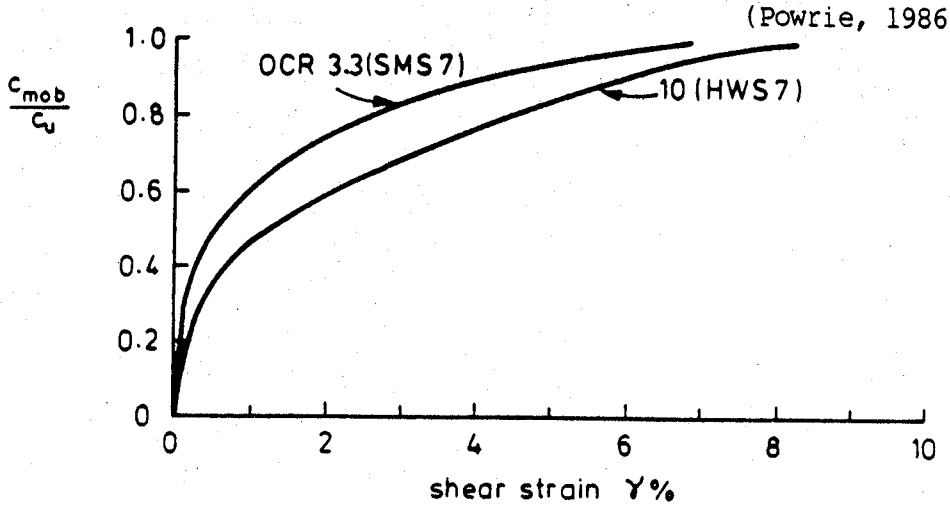

$c_{mob}/c_u = 0.44$. This requires $\gamma = 8.5 \times 10^{-3}$, so the prediction is that $\delta = 8.5 \times 10^{-3} \times 20 / 2 = 85$ mm at prototype scale. Now it will be recalled that the outward movement of the reference point was only about 66 mm directly after construction in test HWS7, so the calculation has been slightly conservative in this case.

It might, of course, be argued that the base of the wall can not be dislocated in the fashion of figure 10: indeed the suppression of the "step" at the reference point O could be taken to be the cause of the backward rotation which accompanied translation in the model. The proposed mechanism is approximate, and intended mainly to enable the designer to decide whether the order of magnitude of soil movements will be acceptable. Adaptations for non-homogeneous, anisotropic soils, and which account more carefully for the normal and shear stresses applied to the clay, are being developed.

EXTENSION TO LATERAL PRESSURE ON PILES

Suppose that the vertical plane OV in figure 10 contains piles of diameter d and center spacing s, which develop average lateral pressure p_{av} due to relative soil-pile displacement. For global equilibrium of plane OV it must follow that

$$\sigma_a - \sigma_p = p_{av}\, d/s = p\, d/s \qquad (1)$$

if the pressure p on the pile were taken to be uniformly distributed with a value calculated at mid-depth. The shear strain in the active and passive triangles will be

$$\gamma = \tfrac{1}{2}(q - \sigma_a)/G \;\; = \tfrac{1}{2}\sigma_p /G \qquad (2)$$

This permits the calculation of the mid-depth soil displacement

$$\delta_s = h\, \gamma /4 \qquad (3)$$

However, elastic analysis (1) of the plane strain displacement of a rigid, adherent disc moving through a medium with shear modulus G_r provides that, for a relative displacement δ_r,

$$p = 5.33\ G_r\ \delta_r/d \tag{4}$$

Taking the same uniform pressure profile on the pile, considered to be perfectly fixed at the clay-sand interface, the pile displacement at mid-depth would be

$$\delta_p = 0.044\ p\ d\ h^4/EI \tag{5}$$

Then the relative displacement of the soil against the pile at mid-depth will be

$$\delta_r = \delta_s - \delta_p \tag{6}$$

Equations 4, 5 and 6 allow an independent assessment of mid-plane lateral soil displacement, for comparison with (3):

$$\delta_s = 0.19\ p\ d/G_r \quad + \quad 0.044\ p\ d\ h^4/EI \tag{7}$$

Substituting (2) into (1) we obtain

$$q = 4\ \gamma\ G + \quad p\ d/s \tag{8}$$

Making a string substitution: (3) for γ, and (7) for δ_s, we get:

$$\frac{p}{q} = \frac{1}{\frac{d}{s} + \frac{0.71\ Gdh^3}{EI} + \frac{3\ G\ d}{G_r h}} \tag{9}$$

This provides a quasi-elastic estimate of lateral pressure on a row of piles, due to the undrained imposition of surcharge. For a uniform elastic material, clearly $G_r = G$. However, for soil which has the non-linear stress-strain curve shown in figure 11, the larger strains near the pile will lead to a secant modulus reduced by a factor of about 2. Taking other values appropriate to the first two increments of load in the prototype of SMS7: $d = 1.27$ m, $s = 4$ m, $h = 6$ m, $G = 800$ kPa, $G_r = 400$kPa, $EI = 5.13 \times 10^6$ kNm^2, equation 9 gives (retaining the same order of terms):

$$p/q = 1\ /\ [0.32 + 0.03 + 1.27] = 0.62$$

This compares with the evidence of the deduced lateral pile pressure from SMS7 in figure 9b, where p appeared to be parabolically distributed with a peak value of p/q very close to unity, and therefore a similar average value to that calculated.

Further model studies and FE analyses are in hand, so that an optimum calculation method can be devised. However, it is already clear that the reduction in soil stiffness due to enhanced strains around the pile is much more significant than its absolute value.

When undrained soil strength c_u is fully mobilized everywhere, plasticity analyses show (5) that the limiting lateral pressure $p_u \simeq 10.5\ c_u \pm 1.35\ c_u$, over the possible range of soil-pile adherence factors. Replacing equation 3 by the plastic alternative

$$q - \sigma_a = \sigma_p = 2c_u \qquad (10)$$

and substituting in equation 1, with $p = 10.5c_u$, we get

$$q = c_u\ (4 + 10.5\ d/s) \qquad (11)$$

The initial quasi-undrained loading phase of test SMS7 is compared in figure 12 with the predictions of equations (9) and (11). The data are compared on normalized axes of q/c_u and p/c_u, where p is the mean pressure inferred to act on the piles in the soft layer, and c_u is the shear strength at the centre of that layer. The calculation is sufficient, in this case, to allow the approximate prediction of lateral pressures in the loading range $q < 4c_u$, within which the undrained settlement might be tolerable.

CONCLUSIONS

1. Lateral displacements of bridge abutments are strongly related to the soil-structure interaction which occurs as backfill is placed. Centrifuge tests of abutments on spread foundations over firm to stiff clay showed an outward displacement during backfilling, which tended to reduce lateral earth pressures towards fully active values. On consolidation, however, the tendency for backward rotation led to a significant increase in earth pressure, albeit with negligible movement at the deck support.

2. Lateral displacements of piled bridge abutments may be significantly underestimated if the lateral loading of the piles themselves, due to squeeze of soft clays under the embankment, is not accounted for. Centrifuge tests of piles subject to surcharge loading showed that lateral pressures could be of the same order of magnitude as the surcharge. These came into effect as soon as the surcharge was placed: subsequent consolidation hardly affected them.

3. It was shown that a geo-structural mechanism comprising two deforming triangles could offer a rationale for the estimation of lateral displacements and pressures, which was sufficiently accurate in the two cases examined to form a basis for design. The feature of the method was its approximate treatment of equilibrium and compatibility which permitted non-linear stress-strain data from appropriate soil tests to be incorporated directly in simple calculations.

Figure 12. Elasto-Plastic Interaction Diagram for Surcharge-Induced Lateral Pressure on a Pile

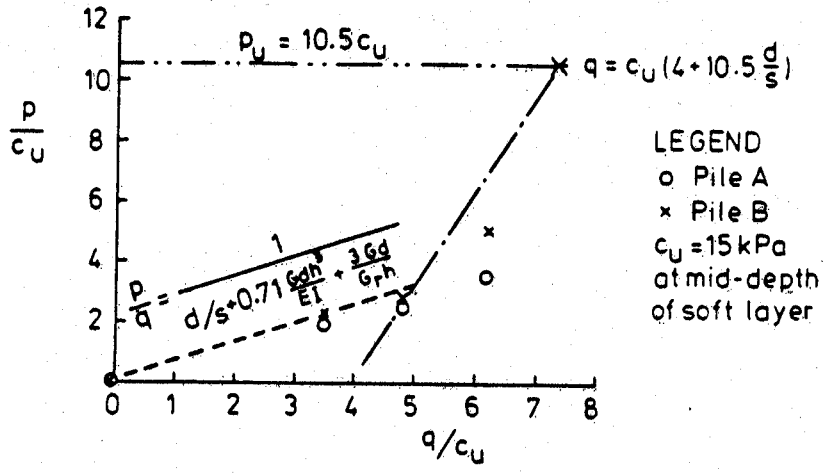

REFERENCES

1. FJ Baguelin, RA Frank & Y Said, Theoretical Study of Reaction Mechanism of Piles, Geotechnique, 27 (3), 1977, 405-434.
2. WH Craig, Installation Studies for Model Piles, Proc. Symp. Applications of Centrifuge Modelling to Geotechnical Design, Univ. of Manchester (UK), 1984, Ed. Craig, Balkema, 440-455.
3. LK Moulton, HVS Ganga Rao & GT Halvorsen, Tolerable Movement Criteria for Highway Bridges, RD-85/107, FHWA, Wash. DC, 1985.
4. W Powrie, The Behaviour of Diaphragm Walls in Clay, Ph.D. Thesis, University of Cambridge (UK), 1986.
5. MF Randolph & GT Houlsby, The Limiting Pressure on a Circular Pile Loaded Laterally in Cohesive Soil, Geotechnique, 34 (4), 1984, 613-623.
6. AN Schofield, Cambridge University Geotechnical Centrifuge Operations, Geotechnique, 30 (3), 1980, 227-268.
7. SM Springman, Lateral Loading on Piles Due to Simulated Embankment Construction, Ph.D. Thesis, University of Cambridge (UK), 1989.
8. HW Sun, Soil Structure Interaction Problem of Retaining Wall on Compressible Foundation, M.Phil Thesis, University of Cambridge (UK), 1987.

ACKNOWLEDGEMENTS

The work described here was supported by research contracts let to the first author by the Transport and Road Research Laboratory of the UK Department of Transport. The opinions expressed here are the authors' and do not necessarily coincide with those of the Laboratory or the Department.

Wing Sun is grateful for the financial support of the Croucher Foundation of Hong Kong, and the Overseas Research Student Award from the CVCP of British Universities.